STANDARD PLANE LOCALIZATION IN ULTRASOUND BY RADIAL COMPONENT

Xin Yang [1,2], *Dong Ni* [1,*], *Jing Qin* [2], *Shengli Li* [3,*], *Tianfu Wang* [1], *Siping Chen* [1], *Pheng Ann Heng* [4]

[1]National-Regional Key Technology Engineering Laboratory for Medical Ultrasound, School of Medicine, Shenzhen University, P. R. China

[2]Center for Human Computer Interaction, Shenzhen Institute of Advanced Integration Technology, P.R.China

[3]Department of Ultrasound, Affiliated Shenzhen Maternal and Child Healthcare Hospital of Nanfang Medical University, P. R. China

[4]Department of Computer Science and Engineering, The Chinese University of Hong Kong, Hong Kong, P. R. China

ABSTRACT

The acquisition of standard planes is crucial for medical ultrasound (US) diagnosis. In this paper, we present a hierarchical supervised learning framework for automatically detecting standard plane in consecutive 2D US images. The technique is demonstrated by developing a system that localizes fetal abdominal standard plane (FASP) from US videos. We first propose a novel radial component-based model (RCM) to describe the geometric constrains of key anatomical structures (KAS). In order to enhance the detection accuracy, we further adopt random forests classifier for detection of KAS within the regions constrained by RCM. Finally, a second-level classifier combines the results of component detectors to identify a US image as a "FASP" or a "nonFASP". Experimental results show that our method significantly outperforms both the full abdomen and the separate anatomy detection methods without geometric constrains.

Index Terms— Ultrasound, Standard plane, Fetal abdomen, Components, Machine learning, Object detection

1. INTRODUCTION

Ultrasound (US) is prevalent in routine clinical examinations and widely used for pregnancy diagnosis. The pipeline of US-based diagnosis includes three sequential steps, namely, scanning, selection of standard planes and diagnosis. Among them, acquisition of standard plane is crucial for following biometric measurements and diagnosis. However, this step requires substantial experience and good knowledge of human anatomy, therefore is very challenging for novices and can be time-consuming and complex even for experienced examiners. It is often cited as one of the inherent disadvantages of US compared to other imaging modalities such as CT and MRI. Hence, the development of automatic methods for localizing standard planes would enhance the ability of non-experts to operate US devices and improve the diagnostic efficiency.

To date, a few works have contributed to the localization of standard planes from 2D US images. Zhang et al. [1] proposed to select standard planes of gestational sac from US videos based on cascade AdaBoost classifier and local context information. Rahmatullah et al. [2] proposed to detect anatomical structures from manually extracted abdominal US images by integration of global and local features. Kwitt et al. [3] proposed to localize target structures from US videos by building kernel dynamic texture (KDT) models and evaluated the methods on phantoms. Some other works [4, 5] presented the automatic classification of echocardiogram view based on dense feature extraction and supervised learning.

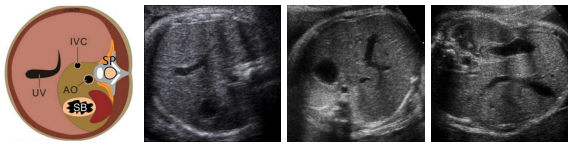

(a) (b) (c) (d)

Fig. 1: (a) Fetal abdominal anatomy, (b)-(d) typical FASPs

Although previous works have illustrated the promising of automatically localizing standard planes from 2D US images, this task remains very challenging due to several reasons. First, as shown in Fig. 1, the fetal abdominal standard plane (FASP) is determined by presence of three key anatomical structures (KAS): stomach bubble (SB), umbilical vein (UV), and spine (SP). However the FASP class often has high intra-class variations due to the artifacts, deformations of KAS, various image intensities, different fetal postures and scanning orientations, which would make it difficult to detect the FASP as a whole. Second, simple detection of KAS separately may not perform well since large numbers of regions appear similar to KAS. For example, shadows, abdominal aorta (AO), inferior vena cava (IVC) and hypoechoic spinal cord are often detected as SB or UV mistakenly.

Recently, component-based methods [6, 7], which search for object by looking for its identifying components rather than the whole object, have been proposed to detect the object composed of multiple components and with high intra-class variability (e.g. people), and proved to be more robust than the full-object detection methods. Inspired by these works, we propose to detect FASPs in consecutive 2D US images by a hierarchical supervised learning framework. First, the region containing abdomen (namely region of interest, ROI)

* Corresponding author: nidong@szu.edu.cn, lishengli63@126.com

is detected using its random forests [8] classifier to reduce the search range. Next, three distinctive component detectors are trained by random forests to find SB, UV and SP within the regions constrained by a novel radial component-based model (RCM), which describes the geometric constrains of key anatomical structures. Finally, a second-level classifier combines the results of component detectors to identify the US image as a "FASP" or a "nonFASP".

2. RANDOM FORESTS CLASSIFIERS

Recently random forests (RF) [8] classifiers have emerged as a novel type of classifier that has several advantages over traditional classifiers [9], such as, the non-parametric nature, high classification accuracy and capability to determine variable importance. In this regard, we propose to adopt random forests to train four classifiers by selecting six types of Haar features [10], each for detecting ROI, SB, SP and UV. In our method, the RF classifier consists of a number of binary decision trees. Each decision tree t is constructed by using a random subset of the training data and recursively creating the nodes that divide the input data into distinct subsets. The splitting stops when a predefined maximal depth is reached, or when the training subset does not contain enough samples. Suppose that D_i is the input training data of one node, the node is trained by finding the parameters of weak classifier that maximize the the information gain (IG) of splitting D_i into D_j and D_k, defined as:

$$IG(D_i, D_j, D_k) = E(D_i) - \frac{|D_j|}{|D_i|}E(D_j) - \frac{|D_k|}{|D_i|}E(D_k) \quad (1)$$

where $E(D_x),\ x = i, j, k$ is the entropy of D_x.

To train the classifiers, positive samples were generated by cropping image regions that contain the anatomical objects while negative samples were extracted randomly from the background and some of them have an overlap of 20% to 40% with a positive sample. Note that the cropped image region was normalized into a square of 80×80 pixels. Once the classifiers are obtained, ROI is first detected from the whole US image by its RF classifier in order to reduce the search range of KAS. While, the other three RF classifiers are used for the component based detection.

3. RADIAL COMPONENT-BASED DETECTION

In component-based detection systems, component model that describes the geometric constraints of components is vital to improve the detection accuracy. Such methods often divide the object into several regions, where components are detected separately, according to the prior knowledge of the object structure, and thus allows for position variations of components. In contrast, a full-abdomen detector employs a fixed representation of the object without taking full advantage of the known geometric properties of the object. For our task, the geometric model of FASP is more complicated than face or people that are the targets studied in [6, 7], due to the complex anatomical structure of FASP, various fetal postures and scanning orientations. In this regard, we propose a novel radial component model (RCM) to describe the geometric relationship of KAS. This model is built based on both the anatomical structure of abdomen (Fig. 1(a)) and the statistical analysis on 850 FASP training images by rotating these images to the standard view shown in Fig. 1(a), which is further validated by one of the authors, an experienced radiologist.

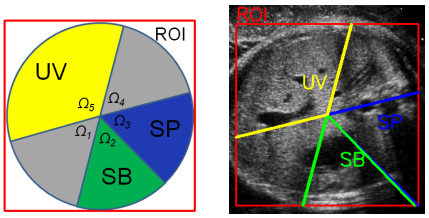

(a) (b)

Fig. 2: (a) RCM, (b) One typical FASP modeled by RCM

As shown in Fig. 2, five radial subregions are divided from the fetal abdomen. The origin of five subregions is located at the center of the ROI, which is detected before the component detection. Suppose the inscribed circle of the square (ROI) is Ω, the five radial subregions are Ω_i, the angle range of each subregion is ϕ_i, specifically the starting angle of Ω_1 is α, RCM can be formulated as

$$\Omega = \cup_{i=1}^{5}\Omega_i, \quad \Omega_j \cap \Omega_k = \emptyset\ (j \neq k) \quad (2)$$

$$\phi_i \in [\alpha + (i-1) * 60^\circ, \alpha + i * 60^\circ]\ (i = 1, 2, 3, 4) \quad (3)$$

$$\phi_5 \in [\alpha + 240^\circ, \alpha + 360^\circ] \quad (4)$$

where $\Omega_2, \Omega_3, \Omega_5$, represent the subregions where SB, SP and UV are most probably located respectively, Ω_1, Ω_4 are the subregions where the KAS are not contained. During the detection stage, the system checks to ensure that the detected anatomies are in the proper geometric configuration. In particular, KAS are only identified by the RF detectors centered in the regions modeled by RCM. It is also worth noting that this detection process is iterative by rotating RCM one constant angle for each iteration, due to various fetal postures and scanning orientations. In this study, the constant angle is set as 20° based on experiments. Besides the advantages mentioned above, our method has several other merits. First, since KAS are detected separately in the constrained regions, the inter-class variability of KAS is increased. Second, false positives with similar appearance to KAS located in regions Ω_1, Ω_4 can be excluded to improve the detection accuracy.

4. FASP DETECTION BY COMBINATION CLASSIFIER

Once the component detectors have been applied to all geometrically permissable regions for each iteration, the highest component scores of each iteration are entered into the data

Table 1: Details of training data.

	Positive	Negative		Positive	Negative		Positive	Negative
ROI	1000	2440	SP	1000	2000	CC	1000	2000
SB	1500	2000	UV	758	2000			

vector that serves as the input of second level classifier, i.e., the combination classifier (CC). The component score is the output of its RF classifier, the combination score is obtained from CC during each iteration, while the final detection score of each image is the maximal combination score of all iterations. Then the US image in the videos with the highest detection score is identified as FASP when the score is above one threshold, which is set as 0.7 based on the experiments. In this study, we adopt the polynomial SVM [11] as the combination classifier. Positive samples are generated by selecting KAS form FASPs and taking the RF score for each anatomy. The procedure of detecting FASP by CC is shown in Fig. 3.

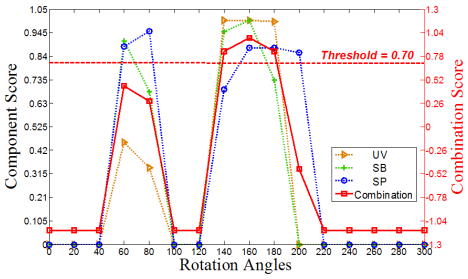

Fig. 3: Illustration of FASP detection by combination classifier. Green, blue and yellow lines represent the component score of SB, SP and UV, respectively, at different iterations. Red line represents the combination score of SVM classifier.

5. EXPERIMENTAL RESULTS AND DISCUSSION

We used 1995 expert annotated fetal US abdomen images for generating the training samples, as shown in Table 1. Besides, 207 fetal abdomen videos containing at least one FASP acquired from 207 pregnant women were used for FASP detection test. Fetal gestational age was from 18 to 40 weeks. All images and videos were acquired using a Siemens Acuson Sequoia 512 US scanner from Shenzhen Maternal and Child Healthcare Hospital. Conventional US sweep was performed to obtain the videos on pregnant women in the supine position. Each sweep lasted approximately 2-6 s and each video contained 17-48 frames. The parameters for all RF classifiers are same and obtained from the experiments. The maximal depth of each tree, the number of trees and the number of features for each node are set as 6, 50 and 340, respectively.

We first evaluated the performance of four RF classifiers on detection of ROI, SB, SP and UV by False Positive Per Window (FPPW) [12]. The ROC curves are shown in Fig. 4. UV performs the best, followed by the SB, SP and ROI. The relative low detection accuracy of ROI may be due to the high intra-class variability caused by a variety of fetal gestational ages and the partially lacking of abdominal contours caused by shadows. As a whole, the results obtained by RF classifiers outperform the results by AdaBoost presented in [2] and illustrate the efficiency of RF.

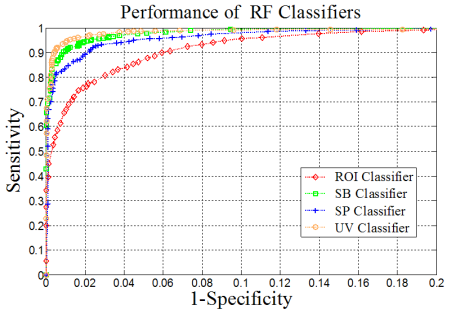

Fig. 4: Performance of four RF classifiers

We then compared the performance of three methods on detecting FASP from US images: the proposed radial component-based detection method (RCD), the full abdomen detection method (FAD), and the separate anatomy detection method (SAD). FAD is based on the full abdomen RF classifier and the sliding window detector is translated and rotated during the detection stage. SAD is a two-level hierarchical detection method, which is similar to the proposed method. However, the anatomy detection is carried out in the whole ROI and not constrained by the geometric model. The ROC curves shown in Fig. 5 illustrate the detection performance of three methods by testing on 992 FASPs and 1600 nonFASPs. In our method, the true and false positive rates are 0.73 and 0.25 respectively when $Threshold = 0.7$. Our proposed method achieves the best detection accuracy and the performance of SAD is relatively better than FAD, which proves that RCM can improve the detection accuracy by making use of the prior knowledge of anatomical structures.

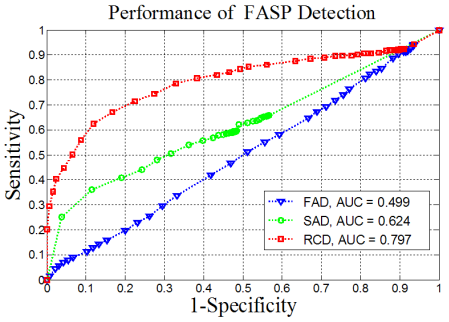

Fig. 5: Performance of detecting FASP from US images

We further compared the performance of three methods on detecting FASP from 207 US vidoes. The correctness of detected FASP was validated by a radiologist with more than five years of experience in obstetrics US. As shown in Fig. 6, we can correctly locate FASP in 50.7%, 55% and 81.6% videos using FAD, SAD and RCD method respectively, further demonstrating the effectiveness of our method. Fig. 7 illustrates the typical examples of FASPs located by three methods. A false FASP (Fig. 7(a)) is selected by FAD method, while from the same video, the true FASP

(Fig. 7(b)) can be localized by our method. Another false FASP (Fig. 7(c)) is located due to the false positive of UV obtained by SAD method while in our method the false positive of UV can be corrected by RCM model, and hence the correct FASP (Fig. 7(d)) is obtained.

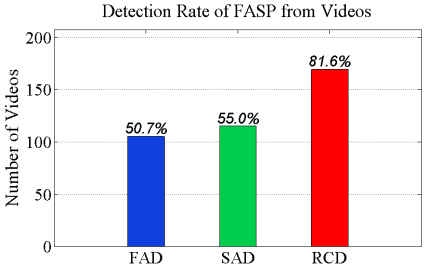

Fig. 6: FASP Detection rate by three methods from US videos

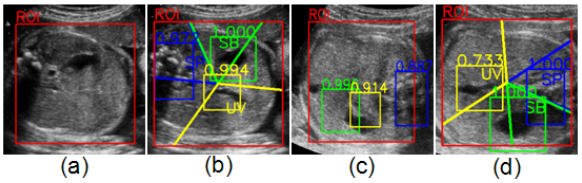

Fig. 7: Typical examples of FASPs located by three methods

6. CONCLUSION

This paper presents an automatic solution for localizing FASP from US videos. We propose a novel radial component-based model to describe the geometric constrains of KAS. This method can handle variations in anatomy positions, and exclude the regions with similar appearance to KAS. We further adopt the RF classifiers to enhance the detection performance of KAS. In addition, we use the second-level SVM classifier to combine the results of component detectors and identify a US image as a "FASP" or a "nonFASP". Experimental results illustrate the efficiency of our proposed method. Our future work will focus on the automatic measurement of abdomen circumference in fetal US based on the detected FASPs and applying the RCM based method to detect other anatomies in medical images.

7. ACKNOWLEDGEMENT

The work described in this paper was supported in part by National Science Foundation of China (No. 61101026, 81270707 and 61233012), in part by Shenzhen Key Basic Research Project (No. 201101013 and JCYJ20130329105033277), in part by Shenzhen-Hong Kong Innovation Circle Funding Program (No. JSE201109150013A), in part by a grant from the Research Grants Council of Hong Kong (No. CUHK412510).

8. REFERENCES

[1] Ling Zhang, Siping Chen, Chien Ting Chin, Tianfu Wang, and Shengli Li, "Intelligent scanning: Automated standard plane selection and biometric measurement of early gestational sac in routine ultrasound examination," *Medical Physics*, vol. 39, no. 8, pp. 5015–5027, 2012.

[2] Bahbibi Rahmatullah, ArisT. Papageorghiou, and J.Alison Noble, "Integration of local and global features for anatomical object detection in ultrasound," in *MICCAI 2012*, vol. 7512, pp. 402–409.

[3] R Kwitt, N Vasconcelos, S Razzaque, and S Aylward, "Localizing target structures in ultrasound video–a phantom study," *Medical Image Analysis*, vol. 17, no. 7, pp. 712 – 722, 2013.

[4] D. Agarwal, K.S. Shriram, and N. Subramanian, "Automatic view classification of echocardiograms using histogram of oriented gradients," in *ISBI 2013*, pp. 1368–1371.

[5] Hui Wu, Dustin M Bowers, Toan T Huynh, and Richard Souvenir, "Echocardiogram view classification using low-level features," in *ISBI 2013*, pp. 752–755.

[6] Anuj Mohan, Constantine Papageorgiou, and Tomaso Poggio, "Example-based object detection in images by components," *Pattern Analysis and Machine Intelligence, IEEE Transactions on*, vol. 23, no. 4, pp. 349–361, 2001.

[7] Pedro F Felzenszwalb, Ross B Girshick, David McAllester, and Deva Ramanan, "Object detection with discriminatively trained part-based models," *Pattern Analysis and Machine Intelligence, IEEE Transactions on*, vol. 32, no. 9, pp. 1627–1645, 2010.

[8] Leo Breiman, "Random forests," *Machine learning*, vol. 45, no. 1, pp. 5–32, 2001.

[9] Antanas Verikas, Adas Gelzinis, and Marija Bacauskiene, "Mining data with random forests: A survey and results of new tests," *Pattern Recognition*, vol. 44, no. 2, pp. 330–349, 2011.

[10] Paul Viola and Michael Jones, "Rapid object detection using a boosted cascade of simple features," in *CVPR 2001*, vol. 1, pp. I–511.

[11] Chih-Chung Chang and Chih-Jen Lin, "Libsvm: a library for support vector machines," *ACM Transactions on Intelligent Systems and Technology (TIST)*, vol. 2, no. 3, pp. 27, 2011.

[12] Navneet Dalal and Bill Triggs, "Histograms of oriented gradients for human detection," in *CVPR 2005*, vol. 1, pp. 886–893.